J|A|C|S ARTICLES

Published on Web 02/05/2010

Development and Application of a Near-Infrared Fluorescence Probe for Oxidative Stress Based on Differential Reactivity of Linked Cyanine Dyes

Daihi Oushiki,[†,‡] Hirotatsu Kojima,[‡,§] Takuya Terai,[†,‡] Makoto Arita,[†] Kenjiro Hanaoka,[†,‡] Yasuteru Urano,[†] and Tetsuo Nagano*[,†,‡,§]

Graduate School of Pharmaceutical Sciences and Chemical Biology Research Initiative, The University of Tokyo, 7-3-1 Hongo, Bunkyo-ku, Tokyo 113-0033, and CREST, Japan Science and Technology Agency, 4-1-8 Honcho, Kawaguchi-shi, Saitama 332-0012, Japan

Received November 30, 2009; E-mail: tlong@mol.f.u-tokyo.ac.jp

Abstract: Reactive oxygen species (ROS) operate as signaling molecules under various physiological conditions, and overproduction of ROS is involved in the pathogenesis of many diseases. Therefore, fluorescent probes for visualizing ROS are promising tools with which to uncover the molecular mechanisms of physiological and pathological processes and might also be useful for diagnosis. Here we describe a novel fluorescence probe, FOSCY-1, operating in the physiologically favorable near-infrared region. The probe consists of two differentially ROS-reactive cyanine dyes connected by a linker; reaction of the more susceptible dye with ROS releases intramolecular fluorescence quenching of the less susceptible dye. We successfully applied this probe to detect ROS produced by HL60 cells and porcine neutrophils and for imaging oxidative stress in a mouse model of peritonitis.

Introduction

Reactive oxygen species (ROS) are important signaling molecules which regulate a wide range of physiological functions, but overproduction of ROS results in oxidative stress and is involved in the pathogenesis of many diseases, including cardiovascular disease, cancer, and neurological disorders.[1−3] Therefore, methods for visualizing ROS would be powerful tools to elucidate the molecular mechanisms that underlie such physiological and pathological conditions and might also be useful for diagnosis.

Various methods for visualizing ROS have been developed.[4−7] Among them, fluorescence imaging methods are generally superior in terms of sensitivity, selectivity, and ease of use. Several groups, including ours, have reported fluorescence probes for ROS based on fluorescein, rhodamine, or BODIPY, which are fluorochromes emitting in the visible region.[8−14] These probes have been widely used for cellular imaging of ROS. However, for imaging in tissues or individuals, fluorochromes whose absorption and emission maxima are in the near-infrared (NIR) region, 650−900 nm, are preferred, because they offer low phototoxicity to cells, minimal interference from hemoglobin absorption, low autofluorescence, and good tissue penetration.[15,16] From these points of view, existing probes have severe limitations for in vivo applications. Therefore, we attempted to develop a novel NIR fluorescence probe for imaging of ROS in vivo.

Among NIR fluorochromes, cyanine dyes have attracted considerable attention, and several functional cyanine probes have recently been developed.[17] Akkaya et al. reported an NIR fluorescence probe for Ca^{2+}, whose fluorescence intensity is controlled by photoinduced electron transfer (PeT).[18] Our group also developed NIR fluorescent probes (DACs) for nitric oxide based on the PeT mechanism.[19] A ratiometric NIR probe for Zn^{2+}, DIPCY, was also designed by our group.[20] Fluorescence modulation of DIPCY is controlled by the difference in the electron-donating ability of

† Graduate School of Pharmaceutical Sciences, The University of Tokyo.
‡ Japan Science and Technology Agency.
§ Chemical Biology Research Initiative, The University of Tokyo.

(1) D'Autréaux, B.; Toledano, M. B. *Nat. Rev. Mol. Cell. Biol.* **2007**, *8*, 813–824.
(2) Valko, M.; Leibfritz, D.; Moncol, J.; Cronin, M. T. D.; Mazur, M.; Telser, J. *Int. J. Biochem. Cell Biol.* **2007**, *39*, 44–84.
(3) Winterbourn, C. C. *Nat. Chem. Biol.* **2008**, *4*, 278–286.
(4) Yamato, M.; Egashira, T.; Utsumi, H. *Free Radical Biol. Med.* **2003**, *35*, 1619–1631.
(5) Armstead, W. M. *Brain Res.* **2001**, *910*, 19–28.
(6) Saito, Y.; Yoshida, Y.; Akazawa, T.; Takahashi, K.; Niki, E. *J. Biol. Chem.* **2003**, *278*, 39428–39434.
(7) Yasui, H.; Sakurai, H. *Biochem. Biophys. Res. Commun.* **2000**, *269*, 131–136.
(8) Soh, N. *Anal. Bioanal. Chem.* **2006**, *386*, 532–543.
(9) Kojima, H.; Nakatsubo, N.; Kikuchi, K.; Kawahara, S.; Kirino, Y.; Nagoshi, H.; Hirata, Y.; Nagano, T. *Anal. Chem.* **1998**, *70*, 2446–2453.
(10) Kenmoku, S.; Urano, Y.; Kojima, H.; Nagano, T. *J. Am. Chem. Soc.* **2007**, *129*, 7313–7318.
(11) Ueno, T.; Urano, Y.; Kojima, H.; Nagano, T. *J. Am. Chem. Soc.* **2006**, *128*, 10640–10641.
(12) Setsukinai, K.; Urano, Y.; Kakinuma, K.; Majima, H. J.; Nagano, T. *J. Biol. Chem.* **2003**, *278*, 3170–3175.
(13) Koide, Y.; Urano, Y.; Kenmoku, S.; Kojima, H.; Nagano, T. *J. Am. Chem. Soc.* **2007**, *129*, 10324–10325.
(14) Maeda, H.; Fukuyasu, Y.; Yoshida, S.; Fukuda, M.; Saeki, K.; Matsuno, H.; Yamauchi, Y.; Yoshida, K.; Hirata, K.; Miyamoto, K. *Angew. Chem., Int. Ed.* **2004**, *43*, 2389–2391.
(15) Weissleder, R.; Ntziachristos, V. *Nat. Med.* **2003**, *9*, 123–128.
(16) Weissleder, R. *Nat. Biotechnol.* **2001**, *19*, 316–317.
(17) Kiyose, K.; Kojima, H.; Nagano, T. *Chem.—Asian J.* **2008**, *3*, 506–515.
(18) Ozmen, B.; Akkaya, E. U. *Tetrahedron Lett.* **2000**, *41*, 9185–9188.
(19) Sasaki, E.; Kojima, H.; Nishimatsu, H.; Urano, Y.; Kikuchi, K.; Hirata, Y.; Nagano, T. *J. Am. Chem. Soc.* **2005**, *127*, 3684–3685.

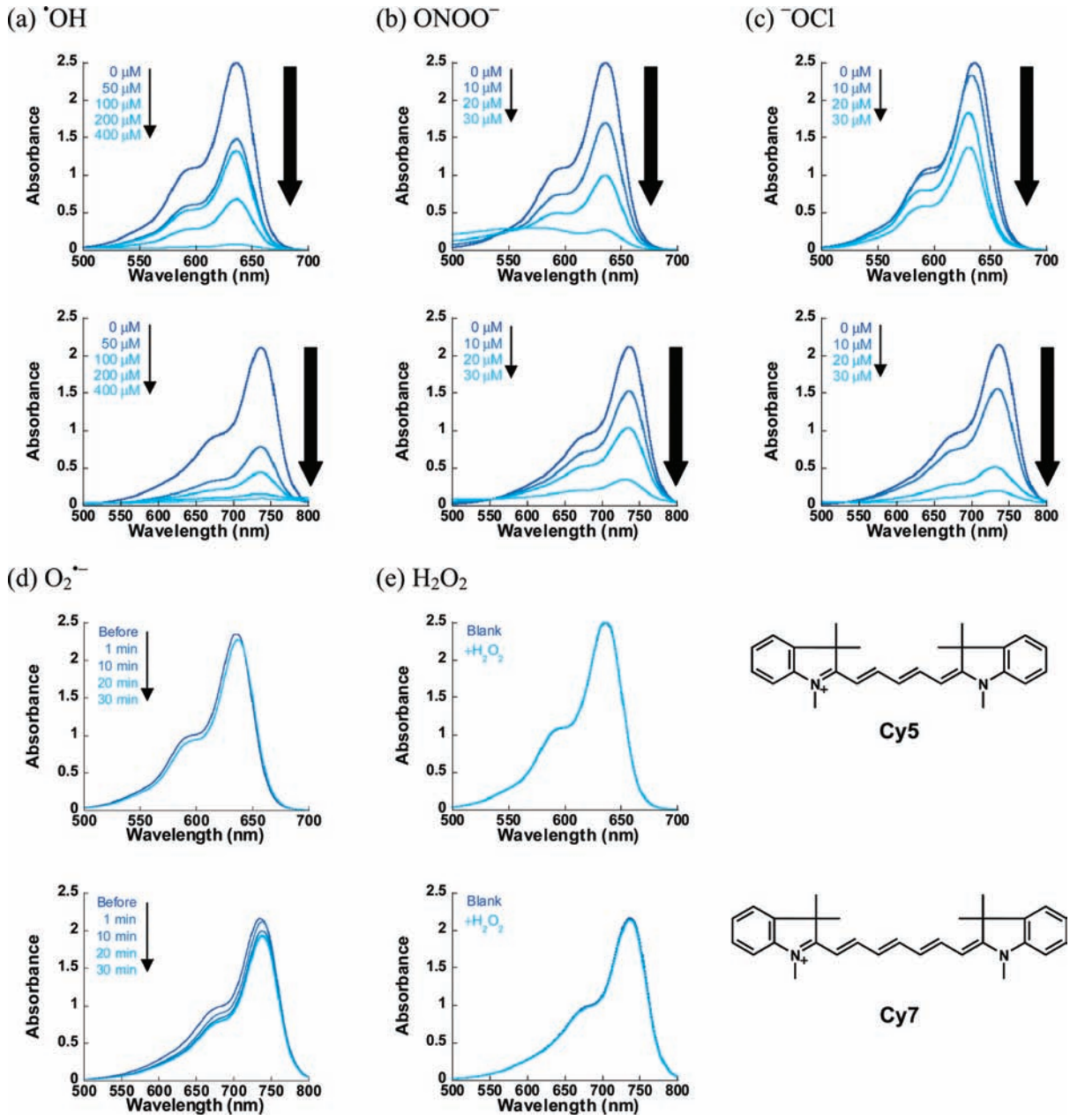

Figure 1. Absorption spectra of a 10 μM solution of Cy5 (upper) or Cy7 (lower) after reaction with various ROS. For details, see the experimental procedure in the Supporting Information.

the amine substituent before and after reaction with Zn^{2+}. Furthermore, activity-based probes have also been developed for diverse enzymes.[21−23] These probes have a fluorochrome connected to a quencher via a linker which is cleaved by the enzyme reaction, releasing the quencher and activating the fluorochrome. However, available design strategies for cyanine dyes are still rather limited. Therefore, we set out to establish a novel design strategy to obtain an NIR ROS probe. It is known that photofading of cyanine dyes is caused mainly by formation of singlet oxygen ($^1O_2$) or superoxide ($O_2^{\bullet-}$).[24−26] The corresponding oxindole or benzothiazolone was identified as the major product of the photofading process, and this indicates that the central polymethine chain was oxidatively cleaved. We hypothesized that other ROS might also react with cyanine dye and reduce its absorption in the NIR region; if this is the case, it would provide a basis for cyanine dyes to be used as an oxidative stress sensor.

During this work, cyanine-based ROS probes based on another strategy were reported by Murthy et al.[27] However, they

(20) Kiyose, K.; Kojima, H.; Urano, Y.; Nagano, T. *J. Am. Chem. Soc.* **2006**, *128*, 6548–6549.
(21) Weissleder, R.; Tung, C.-H.; Mahmood, U.; Bogdanov, A. *Nat. Biotechnol.* **1999**, *17*, 375–378.
(22) Xing, B.; Khanamiryan, A.; Rao, J. *J. Am. Chem. Soc.* **2005**, *127*, 4158–4159.
(23) Blum, G.; von Degenfeld, G.; Merchant, M. J.; Blau, H. M.; Bogyo, M. *Nat. Chem. Biol.* **2007**, *10*, 668–677.
(24) Chen, P.; Li, J.; Qian, Z.; Zheng, D.; Okasaki, T.; Hayami, M. *Dyes Pigm.* **1998**, *37*, 213–222.
(25) Chen, X.; Peng, X.; Cui, A.; Wang, B.; Wang, L.; Zhang, R. *J. Photochem. Photobiol., A* **2006**, *181*, 79–85.
(26) Toutchkine, A.; Nguyen, D.-V.; Hahn, K. M. *Org. Lett.* **2007**, *9*, 2775–2777.
(27) Kundu, K.; Knight, S. F.; Willett, N.; Lee, S.; Taylor, W. R.; Murthy, N. *Angew. Chem., Int. Ed.* **2009**, *48*, 299–303.

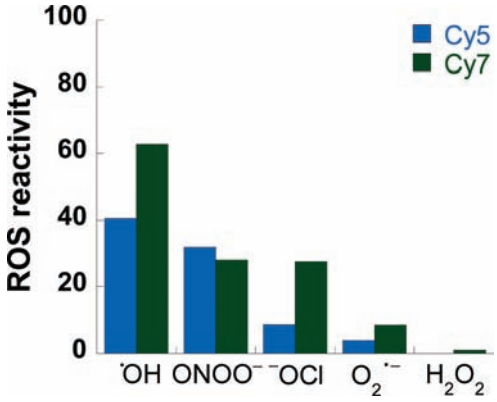

Figure 2. ROS reactivities of Cy5 and Cy7. The dye concentration was 10 μM in 0.1 M phosphate buffer (pH 7.4). $^{\bullet}$OH was generated from H_2O_2 (1 mM) and $Fe(ClO_4)_2$ (50 μM). The $ONOO^-$ concentration was 10 μM. The ^-OCl concentration was 10 μM. $O_2^{\bullet-}$ was generated from XO (4 mU/mL) and xanthine (33 μM). The H_2O_2 concentration was 10 mM.

suffer from background fluorescence increase owing to autoxidation and are sensitive to photooxidation, since they are reduced leuco dyes, like dichlorodihydrofluorescein. It is well-known that the fluorescence intensity of dichlorodihydrofluorescein readily increases during measurement, due to such oxidation.[28]

In this paper, we present a novel ROS-sensitive NIR fluorescence probe based on differential reactivity of cyanine dyes and demonstrate its utility by employing it to image oxidative stress in a mouse model of peritonitis.

Results and Discussion

We first examined whether cyanine dyes themselves react with various ROS. Upon addition of hydroxyl radical ($^{\bullet}$OH), peroxynitrite ($ONOO^-$), or hypochlorite (^-OCl) to a phosphate-buffered solution of commercially available cyanine dyes, Cy5 and Cy7, the absorption of the dyes in the NIR region was lost, while little absorption-spectral change was observed in the presence of $O_2^{\bullet-}$ and hydrogen peroxide (H_2O_2), which are weaker oxidants (Figure 1). We then examined their reactivities with ROS in terms of the percentage absorbance decrease at the maximum wavelength after ROS addition. We found a clear difference of reactivities between Cy5 and Cy7; Cy7 was more susceptible than Cy5 (Figure 2).

Moreover, we analyzed the reaction mixture of Cy7, using an excess of ROS, to ensure that complete reaction occurred. The major product of reaction with every ROS was 1,3,3-trimethyloxindole, indicating that the mechanism of the reaction involves one-electron oxidation of cyanine dyes by ROS, followed by cleavage of the polymethine chain (Figure 3).

Thus, we hypothesized that the reactivities of cyanine dyes with ROS might be correlated with the oxidation potentials. Indeed, the oxidation potential of Cy7 measured by cyclic voltammetry was lower than that of Cy5 (Table 1). We purchased or synthesized a number of cyanine dye derivatives (dyes **1**−**9**; see Figure 4) and examined their reactivities. A plot of ROS reactivities against oxidation potential showed that the oxidation potential of cyanine dyes could be greatly shifted by chemical modification of their structure, and a cyanine dye whose oxidation potential was lower displayed higher ROS reactivity, as we expected (Figure 5 and Table 1). For instance, introduction of a sulfonate group into the indolenine moiety notably suppressed the reactivity, presumably

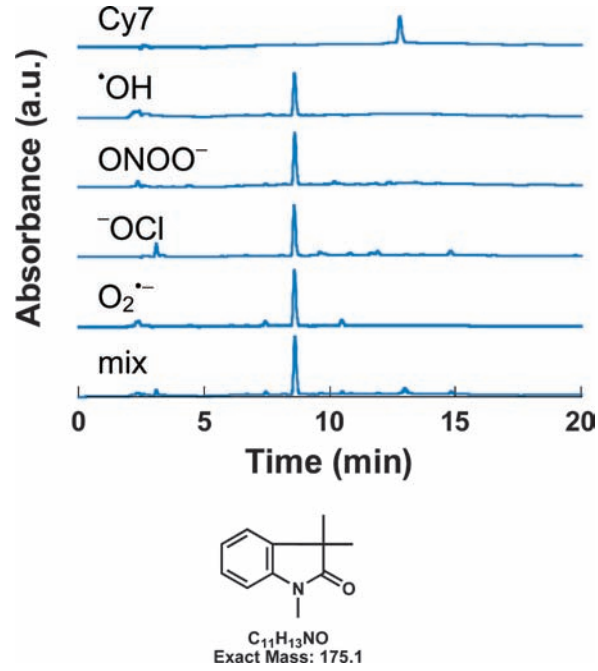

Figure 3. (Top) HPLC chromatograms of (a) Cy7, (b) a reaction mixture of Cy7 with $^{\bullet}$OH, (c) a reaction mixture of Cy7 with $ONOO^-$, (d) a reaction mixture of Cy7 with ^-OCl, (e) a reaction mixture of Cy7 with $O_2^{\bullet-}$, and (f) a mixture of samples (b)−(e). The samples were analyzed by HPLC with linear gradient elution (eluent A/B = 50/50, 10 min, 0/100; flow rate 1.0 mL/min). The monitored wavelength was 250 nm. (Bottom) Structure of 1,3,3-trimethyloxindole. ^{1}H NMR (400 MHz, CD_3OD): δ 7.21−7.17 (m, 2H), 6.99 (td, 1H, J = 7.6, 1.0 Hz), 6.90 (d, 1H, J = 7.6 Hz), 3.12 (s, 3H), 1.24 (s, 6H). ^{13}C NMR (100 MHz, CD_3OD): δ 210.1, 143.6, 137.0, 129.0, 124.1, 123.4, 109.7, 30.7, 26.5, 24.5. HRMS (ESI^+): m/z calcd for $[M+H]^+$, 176.10754; found, 176.10723 (−0.30 mmu).

Table 1. ROS Reactivities of Cyanine Dyes and Their Oxidation Potentials[a]

	$^{\bullet}$OH	$ONOO^-$	^-OCl	$O_2^{\bullet-}$	H_2O_2	E_p (V vs SCE)
IR786S (dye **1**)	82.8	73.8	96.5	72.0	16.9	0.303
Cy7Bn (dye **2**)	86.1	69.5	83.0	0.4	10.4	0.398
IR786 (dye **3**)	82.8	37.3	80.4	35.9	22.8	0.428
Cy7COOH (dye **4**)	41.0	43.9	7.8	12.6	30.4	0.444
Cy7 (dye **5**)	62.7	28.0	27.5	8.4	1.0	0.446
Cy5MeO (dye **6**)	38.7	36.3	21.7	17.0	3.3	0.464
Cy5 (dye **7**)	40.6	31.8	8.5	3.9	0	0.486
Cy5F (dye **8**)	76.8	20.5	16.0	3.3	2.2	0.558
$Cy5SO_3H$ (dye **9**)	13.4	17.7	10.6	0	0	0.628

[a] Cyanine dyes, the structures of which are shown in Figure 4, are numbered from dye **1** to dye **9** in order of their oxidation potential.

because of the strong electron-withdrawing ability of the sulfonate group (see $Cy5SO_3H$ (dye **9**)). On the other hand, Cy7 with thioether at the central carbon of the polymethine chain has such a low oxidation potential that it could react with $O_2^{\bullet-}$ and even with a high concentration of H_2O_2 (see IR786S (dye **1**)). Furthermore, the order of approximate threshold oxidation potentials of reaction with ROS corresponded to that of reduction potentials of ROS, supporting the above reaction mechanism (Figure S1, Supporting Information).[29,30]

Next, we applied these findings to develop a novel NIR fluorescence probe. We focused on the differential reactivity of cyanine dyes and adopted the strategy of utilizing two linked

(28) Hempel, S. L.; Buettner, G. R.; O'Malley, Y. Q.; Wessels, D. A.; Flaherty, D. M. *Free Radical Biol. Med.* **1999**, *27*, 146–159.
(29) Buettner, G. R. *Arch. Biochem. Biophys.* **1993**, *300*, 535–543.
(30) Christophe, K.; Xiuqiong, Z.; Stefan, H.; Reinhard, K.; Willem, H. K. *J. Phys. Chem. A* **2005**, *109*, 965–969.

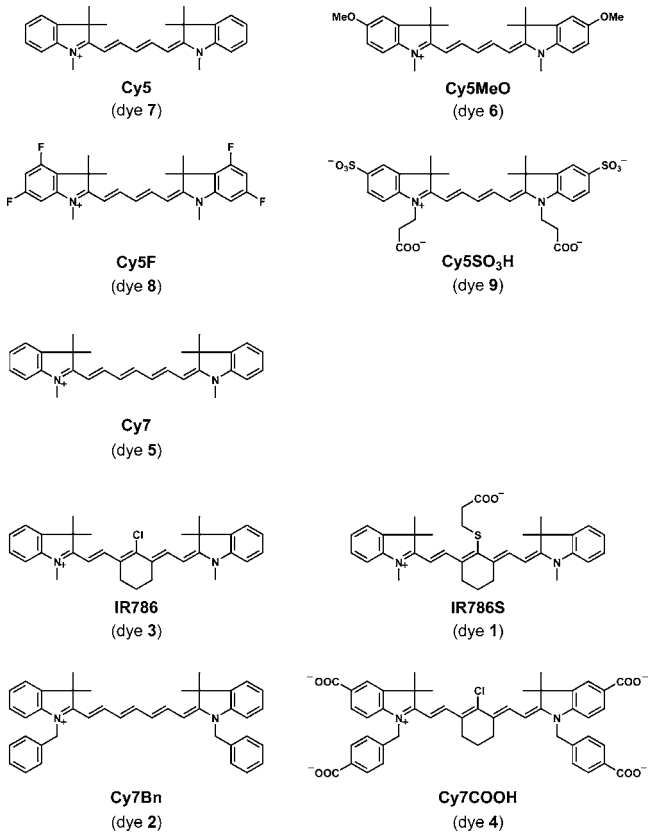

Figure 4. Structures of purchased or synthesized Cy5 derivatives and Cy7 derivatives.

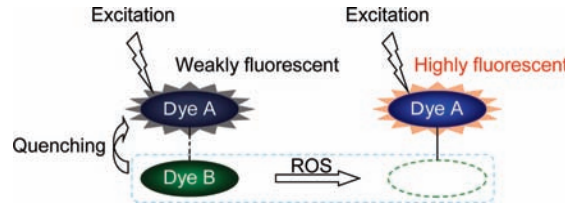

Figure 6. Design strategy utilizing two linked cyanine dyes.

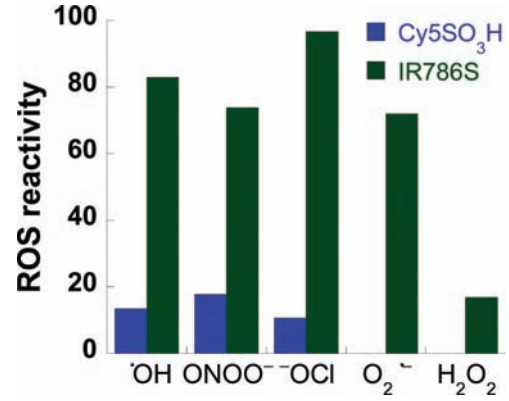

Figure 7. ROS reactivities of $Cy5SO_3H$ (dye **9**) and IR786S (dye **1**). Dye concentrations were 10 μM in 0.1 M phosphate buffer (pH 7.4). $^{\bullet}OH$ was generated from H_2O_2 (1 mM) and $Fe(ClO_4)_2$ (50 μM). The $ONOO^-$ concentration was 10 μM. The ^-OCl concentration was 10 μM. $O_2^{\bullet-}$ was generated from XO (4 mU/mL) and xanthine (33 μM). The H_2O_2 concentration was 10 mM.

cyanine dyes to obtain an oxidative stress sensor. That is, as shown in Figure 6, the designed probe consists of two components, a less ROS-susceptible dye (dye A) as a fluorophore and a highly ROS-susceptible dye (dye B) as an ROS-sensitive fluorescence modulator, connected via a linker. Since the two cyanine dyes are linked to each other with a short separation distance, the fluorescence of dye A should be quenched by the FRET mechanism or by stacking of the two dyes in aqueous solution. However, ROS should break the FRET or stacking by reacting preferentially with the more reactive dye, and consequently fluorescence emission of dye A would then be observed. It should therefore be possible to follow

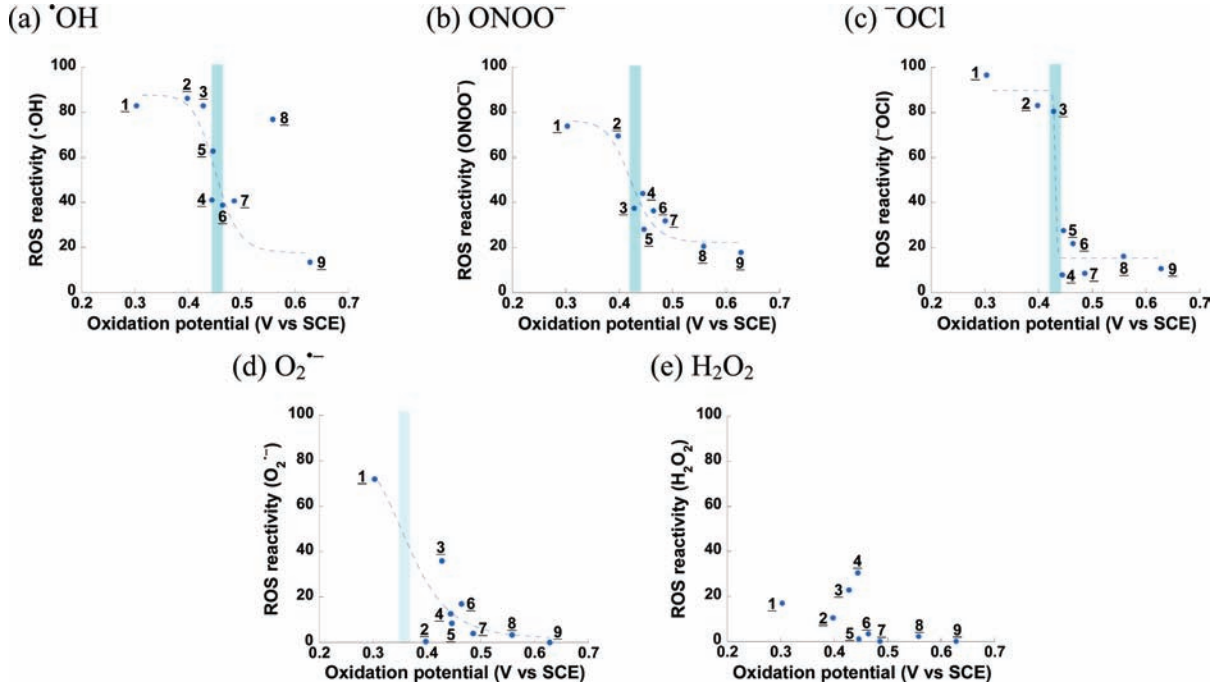

Figure 5. Relationship between the oxidation potentials of cyanine dyes and the reactivities with various ROS. Cyanine dyes are numbered **1**−**9** in the figure. For the structures, see Figure 4.

Scheme 1. Synthesis of FOSCY-1

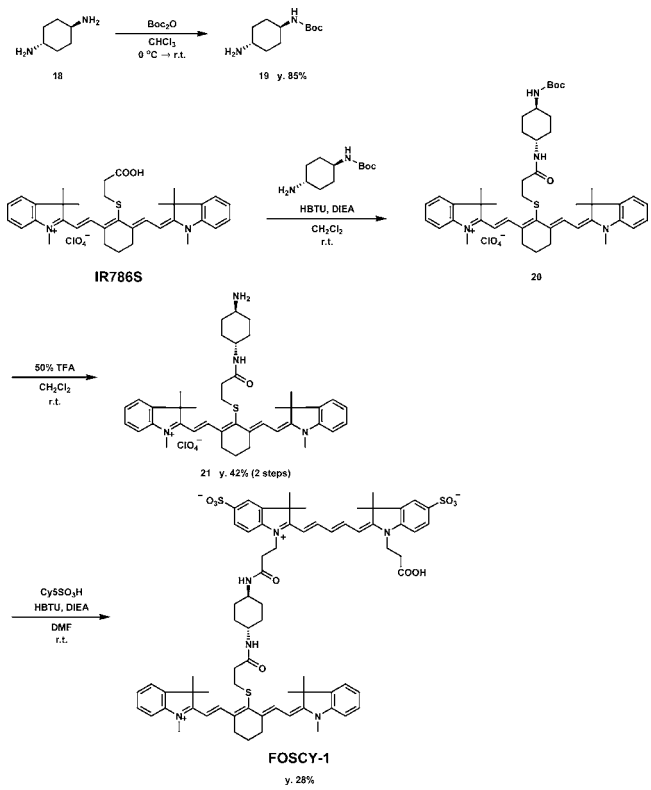

changes in ROS levels by monitoring the fluorescence emission increase of dye A.

Adopting this strategy, we aimed to select the most suitable pair with respect to reactivity. That is to say, ROS should react only with the ROS-sensitive fluorescence modulator. IR786S (dye **1**) and $Cy5SO_3H$ (dye **9**) showed a large difference in ROS reactivity (Figure 7), and IR786S (dye **1**) actually reacted preferentially with ROS in the presence of equal amounts of the two dyes (Figure S2, Supporting Information). Moreover, IR786S (dye **1**) could react even with $O_2^{\bullet-}$, which is particularly important, because this is considered to be the primary ROS which interacts with other molecules to generate other ROS. Therefore, a probe which can detect $O_2^{\bullet-}$ in the NIR region should be very desirable for biological applications, as noted above. Thus, we decided to adopt these dyes and to link them through a cyclohexanediamine linker, affording the candidate sensor FOSCY-1 (Scheme 1).[31]

The absorption and fluorescence spectra of FOSCY-1 measured in phosphate buffer are shown in Figure 8. Two absorption peaks at 644 and 792 nm were observed, indicating the presence of $Cy5SO_3H$ and IR786S, respectively (see Table 2). It appeared that these dyes form a ground-state complex, since the absorption peak of IR786S was red-shifted by about 20 nm.[32] Further evidence for intramolecular interaction was provided by the fluorescence spectra. FOSCY-1 was weakly fluorescent (ϕ_{fl} = 0.014; see Table 2) after excitation of the $Cy5SO_3H$ moiety at 645 nm, and no significant emission corresponding to IR786S fluorescence was observed. In addition, the fluorescence quantum yield of FOSCY-1 after excitation of the IR786S moiety at 771 nm (ϕ_{fl} = 0.009; see Table 2) was also lower than that of free IR786S (ϕ_{fl} = 0.035; see Table 2). These results indicate that the fluorescence of FOSCY-1 is controlled not by the FRET mechanism, but by static quenching.

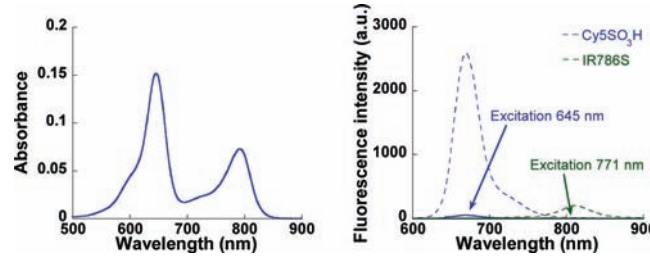

Figure 8. Absorption (left) and fluorescence (right) spectra of FOSCY-1 in 0.1 M phosphate buffer (pH 7.4).

Table 2. Photochemical Properties of $Cy5SO_3H$, IR786S, and FOSCY-1

dye	abs max[a] (nm)	ϵ[a] (10^5 M^{-1} cm^{-1})	emission max[a] (nm)	ϕ_{fl}
$Cy5SO_3H$	646	2.0	671	0.171[b]
IR786S	771	1.1	810	0.035[c]
FOSCY-1	644, 792	1.5 (644 nm)	668 (ex 645 nm)	0.014 (ex 645 nm)[b]
		0.7 (792 nm)	813 (ex 771 nm)	0.009 (ex 771 nm)[c]

[a] Measured in phosphate buffer (0.1 M, pH 7.4). [b] ϕ_{fl} is the relative fluorescence quantum yield estimated by using cresyl violet in MeOH (0.54) (SR1) as a fluorescence standard. [c] ϕ_{fl} is the relative fluorescence quantum yield estimated by using ICG in DMSO (0.13) (SR2) as a fluorescence standard.

Table 3. Maximum Ratio (F/F_0) of the Fluorescence Intensity after ROS Addition (F) to the Initial Fluorescence Intensity (F_0)

$^{\bullet}OH$	$ONOO^-$	^-OCl	$^1O_2$	$O_2^{\bullet-}$	H_2O_2
10.3	14.1	9.6	3.7	5.9	1.1

Therefore, we thought FOSCY-1 could be used as an off/on sensor and examined the reactivities of FOSCY-1 with a variety of chemically and enzymatically generated ROS. As shown in Table 3, FOSCY-1 exhibited a high response to $^{\bullet}OH$, $ONOO^-$, ^-OCl, $^1O_2$, and even $O_2^{\bullet-}$, showing an immediate, concentration-dependent fluorescence enhancement, whereas little increase of fluorescence was observed upon reaction with H_2O_2 (see also Figures S3 and S4, Supporting Information). The results are consistent with the reactivities of IR786S (dye **1**) alone and suggest that the IR786S moiety of FOSCY-1 reacts preferentially with ROS, with loss of quenching, as we had expected. Oxindole formation from the IR786S moiety was confirmed by HPLC analysis (Figure S5, Supporting Information). Moreover, the absorbance and fluorescence of FOSCY-1 were sufficiently stable for practical use with respect to pH change or photooxidation, indicating that FOSCY-1 could detect ROS with high reliability (Figure 9). Thus, FOSCY-1 should be applicable for detection of ROS in chemical and enzymatic systems.

We then applied FOSCY-1 to detect ROS produced by living cells to examine its practical utility as a biological sensor. FOSCY-1 is suitable for the detection of extracellular ROS, since it appears to be almost membrane-impermeable (Figure S6, Supporting Information). We therefore attempted to use FOSCY-1 for detection of ROS involvement in intercellular signaling. HL60 cells are a human promyelocytic leukemia cell line and express both membranous and cytoplasmic NADPH

(31) Takakusa, H.; Kikuchi, K.; Urano, Y.; Kojima, H.; Nagano, T. *Chem.—Eur. J.* **2003**, *9*, 1479–1485.
(32) Johansson, M. K.; Cook, R. M. *Chem.—Eur. J.* **2003**, *9*, 3466–3471.

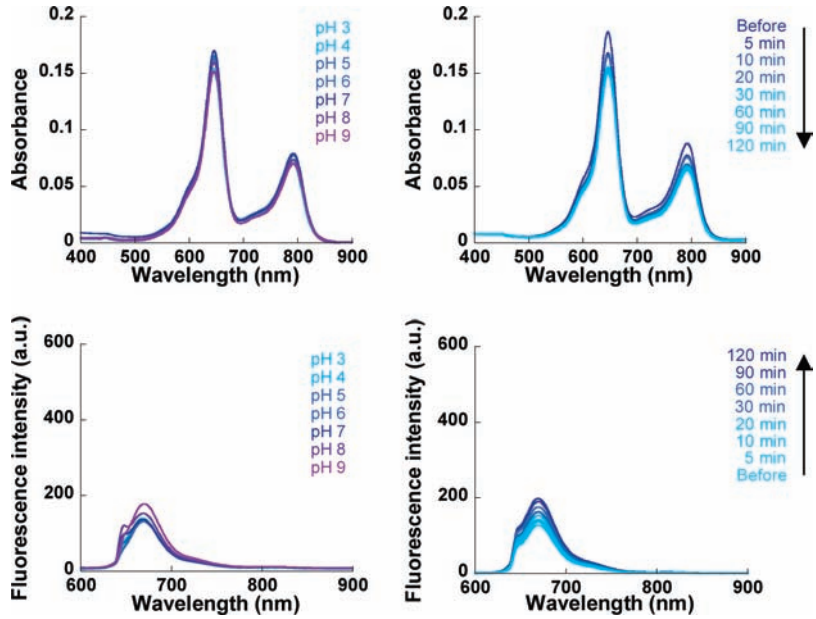

Figure 9. Absorption (upper) and fluorescence (lower) spectral change of FOSCY-1 in phosphate buffer at various pH values (left) or after light irradiation (right, 645 nm, 1.0 mW/cm^2). For details, see the experimental procedure in the Supporting Information.

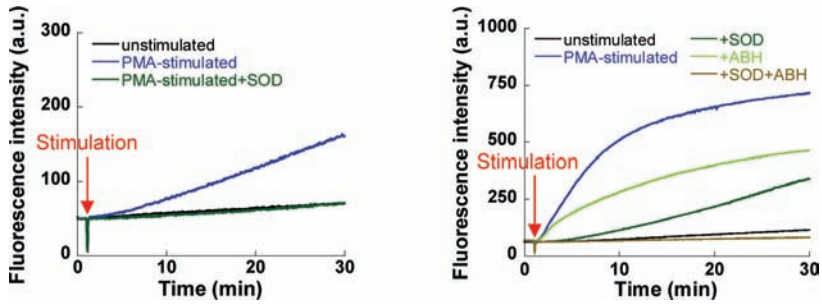

Figure 10. Time courses of fluorescence intensity observed with FOSCY-1 in the presence of PMA-stimulated HL60 cells (left) or porcine neutrophils (right). Representative data are shown ($n = 8$ for HL60 cells or $n = 3$ for porcine neutrophils).

oxidase (NOX) subunits.[33,34] Upon stimulation of the cells with phorbol myristate acetate (PMA) the subunits assemble at the plasma membrane and $O_2^{\bullet-}$ is released by one-electron reduction of oxygen into the extracellular environment. HL60 cells incubated at 37 °C with FOSCY-1 were stimulated with PMA. As shown in Figure 10, the fluorescence intensity of FOSCY-1 gradually increased following cell stimulation, and this increase was almost wholly suppressed by addition of superoxide dismutase (SOD). The results indicated that FOSCY-1 can detect $O_2^{\bullet-}$ generation by HL60 cells. We also examined ROS production by porcine neutrophils. Neutrophils are well-known to generate ROS for host defense and contain NOX and myeloperoxidase (MPO), which catalyzes the formation of $^{-}$OCl from H_2O_2 as ROS-forming enzymes.[35] We found that the fluorescence intensity of FOSCY-1 similarly showed remarkable enhancement following stimulation of neutrophils with PMA (Figure 10). Furthermore, this enhancement was partially suppressed by the addition of SOD or *p*-aminobenzohydrazide (ABH),[36] which is an MPO inhibitor, indicating that FOSCY-1 can detect $O_2^{\bullet-}$ and $^{-}$OCl generation by neutrophils. Indeed, essentially no fluorescence enhancement was observed with PMA-stimulated neutrophils in the presence of both SOD and ABH. These experiments demonstrate that FOSCY-1 is able to detect ROS in a living cellular system.

We also investigated the ability of FOSCY-1 to image oxidative stress in a mouse model of peritonitis. C57Bl/6 mice were given an intraperitoneal (ip) injection of zymosan derived from *Saccharomyces cerevisiae* to induce peritonitis. After 4 h, the mice were anaesthetized, and their abdominal fur was removed. Then, the mice were injected ip with FOSCY-1 and divided into four groups. One group was injected ip with PMA, the second group was injected with saline, and the third and the fourth groups were injected with apocynin (400 μM and 4 mM), which is an NOX inhibitor, followed by PMA. Images were acquired for 60 min by using an in vivo imaging system, MAESTRO. As shown in Figure 11, the fluorescence intensity of FOSCY-1 was remarkably increased by PMA stimulation. This fluorescence enhancement was hardly observed in saline-treated mice and was partially suppressed in a concentration-dependent manner by apocynin treatment (Figures 12 and S7, Supporting Information). Moreover, in vitro experiments using peritoneal exudate cells obtained from these mice showed the same outcome as the in vivo imaging (Figure S8, Supporting Information). Taken together, these experiments demonstrate that FOSCY-1 is applicable for in vivo imaging of oxidative stress.

(33) Teufelhofer, O.; Weiss, R.-M.; Parzefall, W.; Schulte-Hermann, R.; Micksche, M.; Berger, W.; Elbling, L. *Toxicol. Sci.* **2003**, *76*, 376–383.
(34) Dong, J.-M.; Zhao, S.-G.; Huang, G.-Y.; Liu, Q. *Free Radical Res.* **2004**, *38*, 629–637.
(35) Babior, B. M. *Blood* **1984**, *64*, 959–966.
(36) Kettle, A. J.; Gedye, C. A.; Winterbourn, C. C. *Biochem. J.* **1997**, *321*, 503–508.

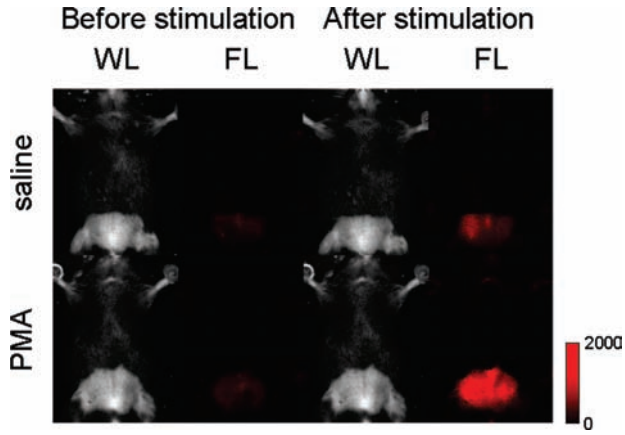

Figure 11. Comparison of white light (WL) and fluorescence (FL) images of the PMA-stimulated peritonitis model mouse (lower, "PMA") and unstimulated peritonitis model mouse (upper, "saline"). Representative data are shown ($n = 6$).

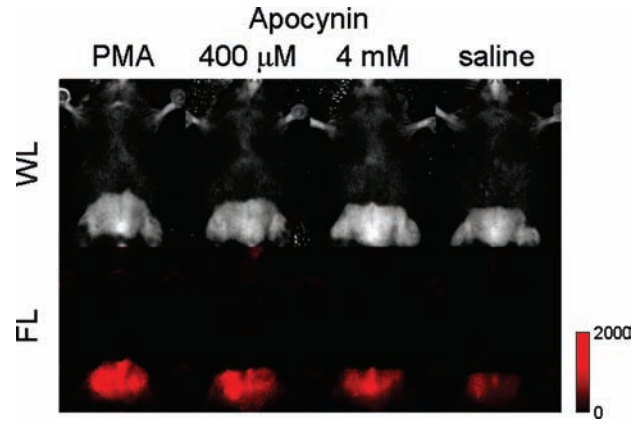

Figure 12. Comparison of white light (WL) and fluorescence (FL) images of apocynin-treated mice (middle, "Apocynin 400 μM" and "Apocynin 4 mM") and nontreated mice (edges, "PMA" and "saline"). Representative data are shown ($n = 3$).

Conclusions

Oxidative stress induced by overproduction of ROS is considered to be involved in the pathogenesis of many diseases. Therefore, imaging of oxidative stress, particularly in vivo, is important in studying the mechanisms of such diseases.

Cyanine dyes are well-known fluorochromes in the NIR region, but their chemical properties have not been thoroughly investigated. We found that cyanine dyes react with ROS and their reactivities are correlated with their oxidation potentials, which can be controlled by chemical modification of their structure. We focused on these characteristics and succeeded in developing FOSCY-1 as a near-infrared fluorescence probe for oxidative stress by linking two cyanine dyes having differential reactivity with ROS; reaction of the more susceptible dye releases fluorescence quenching of the other dye. FOSCY-1 could detect a wide range of physiologically important ROS and could image oxidative stress in a mouse model of peritonitis. On the basis of these results, we anticipate that FOSCY-1 will find wide application as a research tool.

Acknowledgment. This work was in part supported by a Grant-in-Aid for JSPS Fellows (to D.O.), by the Ministry of Education, Culture, Sports, Science and Technology of Japan (Grant Nos. 20689003 to H.K., 19205021 and 20117003 to Y.U., and 20689001 and 21659024 to K.H), and by the Industrial Technology Research Grant Program in 2009 from the New Energy and Industrial Technology Development Organization (NEDO) of Japan (to T.T.). H.K. was also supported by the Sankyo Foundation of Life Science. K.H. was also supported by the Mochida Memorial Foundation for Medical Pharmaceutical Research and Sankyo Foundation of Life Science.

Supporting Information Available: Experimental procedure, synthesis description, and supporting figures. This material is available free of charge via the Internet at http://pubs.acs.org.

JA910090V